

Low-Reynolds-number turbulent forced-convection flow over graded baffle plates

Younes Menni *, Chafika Zidani, Ahmed Azzi and Boumediene Benyoucef

Unit of Research on Materials and Renewable Energies, URMER
Department of Physics, Faculty of Sciences,
Abou Bekr Belkaid University, B.P. 119-13000-Tlemcen, Algeria

(reçu le 26 janvier 2016 – accepté le 28 Avril 2016)

Abstract - *The thermo-hydraulic behaviors of turbulent forced-convection heat transfer flow over a rectangular cross section baffled channel are numerically examined in various graded baffle plate ratio configurations 'GBR = 0.10, 0.11, 0.12, 0.13, 0.14, and 0.15) at different Reynolds numbers, ranging from 12,000 to 32,000. The governing equations that describe the flow are integrated by the finite volumes method, in two dimensions, employing the Commercial CFD software FLUENT 6.3 with low-Reynolds-number $k-\epsilon$ model to describe the turbulence. The velocity and pressure terms of momentum equations are solved with SIMPLE-algorithm. In particular, axial velocity, turbulence intensity, pressure, and temperature fields, average Nusselt number and friction loss are obtained. The numerical runs are carried out for different values of Reynolds numbers and graded baffle ratios at constant wall temperature condition along the top and bottom walls. Results were compared with available experimental data from the literature and good agreement is obtained.*

Résumé - *Ce travail consiste à l'étude numérique du comportement dynamique et thermique de l'écoulement bidimensionnel et du transfert de chaleur turbulent en convection forcée. L'application se fait dans un canal de section rectangulaire muni de chicanes gradées 'GBR = 0.10, 0.11, 0.12, 0.13, 0.14, and 0.15' dont les parois supérieure et inférieure sont maintenues à une température constante. Les équations gouvernantes, basées sur le modèle $k-\epsilon$ à bas nombre de Reynolds sont résolues par la méthode des volumes finis à l'aide de l'algorithme SIMPLE. Le code du calcul numérique en dynamique des fluides FLUENT 6.3 est appliqué pour intégrer ces équations sur chaque volume de contrôle. Les calculs sont effectués pour un nombre de Reynolds compris entre 12,000 et 32,000. En particulier, les champs de vitesse axiale, intensité de turbulence, pression, et de température, le nombre de Nusselt moyen et ainsi que les pertes de charge par frottement sont obtenus. Les résultats numériques sont comparés à ceux obtenus par l'expérience dans la littérature. Cette comparaison montre qu'il y a une bonne concordance avec les données disponibles dans la littérature.*

Key-words: CFD - Graded baffle - In-line arrangement - Rectangular channel - Steady state - Turbulent flow.

1. INTRODUCTION

The use of baffles and fins in channels is commonly used for passive heat transfer enhancement strategy in single phase internal flow. Considering the rapid increase in energy demand, effective heat transfer enhancement techniques have become important task worldwide. Some of the applications of passive heat transfer enhancement strategies are in process industries, thermal regenerator, shell and tube type heat exchanger, internal cooling system of gas turbine blades, radiators for space vehicles and automobiles, etc.

* menni_younes@yahoo.fr

The baffles and fins submitted to laminar and turbulent flows have been analyzed in the recent years by several authors, using numerical and/or experimental techniques. In those studies, different aspect ratio channels [1] and different numbers [2, 3], sizes [4-7], positions [8-11], orientations [12, 13], types [14-19] and shapes [20-27] of baffles were used. All these techniques increase the thermal transfer rate but created catastrophic pressure losses. The purpose of this paper is to investigate, at low-Reynolds-number, the fluid flow and heat transfer characteristics in a constant temperature-surfaced rectangular channel, where the turbulent flow is deflected by in-line baffle plates at graded height according to the channel length.

2. MATHEMATICAL MODELING

2.1 Present geometry

Fluid flow and heat transfer characteristics are analyzed for a constant property fluid flowing turbulently through a two-dimensional horizontal rectangular cross section channel with six lower wall-mounted baffle plates and a constant temperature along both walls, as shown in figure 1. The flow field in the channel is assumed to be steady, incompressible and turbulent, and the fluid is assumed to be Newtonian with constant properties.

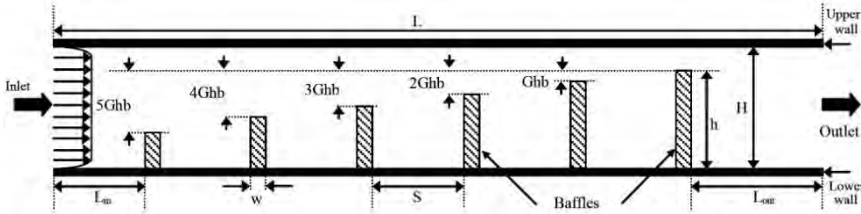


Fig. 1: The geometry of the system under investigation

Table 1 indicates the important parameters of the system. To investigate a geometry effect of the interaction between baffles, the gradation of baffle ratio, Ghb / H is varied in a range of $GBR = 0.10$ to 0.15 in the present simulation.

Table 1: Detailed geometric parameters of the computation domain

Parameter [Unit- m]	Value
Channel length, L	0.554
Channel height, H	0.146
Channel width, W	0.193
Hydraulic diameter, D_h	0.167
Baffle thickness, w	0.01
Baffle height, h	0.12
Spacing, S	0.066
Inlet distance, L_{in}	0.066
Outlet distance, L_{out}	0.098

2.2 Governing equations

The numerical model for fluid flow and heat transfer in the channel was developed under the following assumptions:

- (i) Steady two-dimensional fluid flow and heat transfer.
- (ii) The flow is turbulent and incompressible.

- (iii) Constant fluid properties.
- (iv) Body forces and viscous dissipation are ignored.
- (v) Negligible radiation heat transfer.

Based on the above assumptions, the channel flow is governed by the continuity, the Navier-Stokes equations and the energy equation. The two-equation low-Reynolds-number $k-\varepsilon$ turbulence model, based on Jones *et al.* [28] is employed to simulate the turbulent transport quantities and close the solving problem. In the Cartesian coordinate these equations can be written in the following compact form:

$$\frac{\partial}{\partial x}(\rho \cdot u \cdot \phi) + \frac{\partial}{\partial y}(\rho \cdot v \cdot \phi) = \frac{\partial}{\partial x} \left(\Gamma_\phi \frac{\partial \phi}{\partial x} \right) + \frac{\partial}{\partial y} \left(\Gamma_\phi \frac{\partial \phi}{\partial y} \right) + S_\phi \quad (1)$$

where, ϕ is universal variable responding temperature T , velocity components u and v as well as turbulence parameters k and ε ; u is horizontal component velocity; v is vertical velocity; Γ_ϕ and S_ϕ generalized diffusion coefficient and generalized source term respectively; ρ is the density of the fluid passing through the channel; ν the kinematic viscosity; and ϕ , Γ_ϕ and S_ϕ are given by:

Continuity equation

$$\phi = 1 \quad (2)$$

$$\Gamma_\phi = 0 \quad (3)$$

$$S_\phi = 0 \quad (4)$$

Momentum equation in X-direction

$$\phi = u \quad (5)$$

$$\Gamma_\phi = \mu_e \quad (6)$$

$$S_\phi = -\frac{\partial p}{\partial x} + \frac{\partial}{\partial x} \left(\mu_e \left(\frac{\partial u}{\partial x} \right) \right) + \frac{\partial}{\partial y} \left(\mu_e \left(\frac{\partial v}{\partial x} \right) \right) \quad (7)$$

Momentum equation in Y-direction

$$\phi = v \quad (8)$$

$$\Gamma_\phi = \mu_e \quad (9)$$

$$S_\phi = -\frac{\partial p}{\partial y} + \frac{\partial}{\partial x} \left(\mu_e \left(\frac{\partial u}{\partial y} \right) \right) + \frac{\partial}{\partial y} \left(\mu_e \left(\frac{\partial v}{\partial y} \right) \right) \quad (10)$$

Energy equation

$$\phi = T \quad (11)$$

$$\Gamma_\phi = \mu_e / \sigma_\tau \quad (12)$$

$$S_\phi = 0 \quad (13)$$

k-turbulent kinetic energy equation

$$\phi = k \quad (14)$$

$$\Gamma_\phi = \mu_t + \mu_t / \sigma_k \quad (15)$$

$$S_\phi = -\rho \cdot \varepsilon + G \quad (16)$$

ε -turbulent dissipation rate equation

$$\phi = \varepsilon \quad (17)$$

$$\Gamma_\phi = \mu_t + \mu_t / \sigma_\varepsilon \quad (18)$$

$$S_\phi = (C_{1\varepsilon} f_1 G - C_{2\varepsilon} f_2 \rho \cdot \varepsilon) \cdot \varepsilon / k \quad (19)$$

With

$$G = \mu_t \times \left\{ 2 \left(\frac{\partial u}{\partial x} \right)^2 + 2 \left(\frac{\partial u}{\partial y} \right)^2 + \left(\frac{\partial v}{\partial x} + \frac{\partial u}{\partial y} \right)^2 \right\} \quad (20)$$

$$\mu_e = \mu_l + \mu_t \quad (21)$$

$$\mu_t = f_\mu \cdot \rho \cdot C_\mu \cdot k^2 / \varepsilon \quad (22)$$

The turbulent constants in above equations were adopted in accordance with those of Launder *et al.* [29], and Chieng *et al.* [30]. They are shown in **Table 2**.

Table 1: Turbulent constants in the governing equations

Constant	$C_{1\varepsilon}=C_{3\varepsilon}$	$C_{2\varepsilon}$	C_μ	σ_k	σ_ε	σ_T
Value	1.44	1.92	0.09	1.00	1.30	0.90

In the version of Versteeg *et al.* [31], the modeling damping functions f_1 , f_2 and f_u used for the LRN $k-\varepsilon$ model are presented as:

$$f_u = \left(1 - \exp(1 - 0.0165 R_y) \right)^2 (1 + 20.5 / R_T) \quad (23)$$

$$f_1 = 1 + (0.5 / f_u)^3 \quad (24)$$

$$f_2 = 1 - \exp(-R_T^2) \quad (25)$$

where

$$R_T = \frac{\rho \cdot k^2}{\varepsilon \cdot \mu} \quad \text{and} \quad R_y = \frac{\rho \cdot \sqrt{k} \cdot y}{\mu} \quad (26)$$

The damping function, f_u , which is a function of dimensionless wall-normal distance. $y^+ = y\sqrt{k}/\nu$, is used to model the damping effect associated with pressure-strain correlations in the vicinity of walls.

2.3 Boundary conditions

The numerical simulations are conducted in a two-dimensional domain, which represents a graded baffled channel of 0.167 m hydraulic diameter and 0.554 m length. Air is the working fluid with the flow rate in terms of Reynolds numbers ranging from 12000 to 32000. In the entrance region, a uniform one-dimensional velocity profile was prescribed, as shown in figure 1. The pressure at the inlet of the computational domain was set equal to the zero (gauge) while the turbulence intensity was kept at 2%. The kinetic energy of turbulence and dissipation rates are prescribed, respectively, as

$$k_{in} = 0.005 U_{in}^2 \quad (27)$$

$$\epsilon_{in} = 0.1 k_{in}^2 \tag{28}$$

A constant temperature of 102 °C (375 K) was applied on the entire wall of the computational domain as the thermal boundary condition. The temperature of the working fluid was set equal to 27 °C (300 K) at the inlet of the channel. Besides, non-slip and impermeability boundary conditions are imposed at the walls. At the solid-fluid interfaces it is imposed,

$$T_f = T_s \tag{29}$$

$$\lambda_f \frac{\partial T_f}{\partial x} = \lambda_s \frac{\partial T_s}{\partial x} \tag{30}$$

where, λ_f and λ_s are fluid thermal conductivity and solid thermal conductivity, respectively. In the channel outlet it is prescribed the atmospheric pressure, and all gradients are assumed to be zero. The Reynolds number, calculated with the hydraulic diameter of the channel, D_h , and the reference velocity, \bar{U} , is taken according to the experiments of Demartini *et al.*, [21], it is equal to 8.73×10^4 . This dimensionless parameter is defined as

$$Re = \frac{\rho \bar{U} D_h}{\mu} \tag{31}$$

The skin friction coefficient, C_f is given by

$$C_f = \frac{\tau_w}{1/2 \rho \cdot \bar{U}^2} \tag{32}$$

The friction factor, f , is computed by pressure drop, ΔP , across the length of the rectangular channel, L , as:

$$f = \frac{(\Delta P / L) \cdot D_h}{1/2 \rho \cdot \bar{U}^2} \tag{33}$$

The friction factor, f_0 , in a fully developed smooth channel at the same Reynolds number can be presented as [32]:

$$f_0 = \frac{1}{(0.79 \ln Re - 1.64)^2} \quad \text{for} \quad 3000 \leq Re \leq 5 \times 10^6 \tag{34}$$

The local and average convective Nusselt numbers are defined,

$$Nu_x = \frac{h_x D_h}{\lambda_f} \tag{35}$$

$$Nu_{av} = \frac{1}{L} \int Nu_x \partial x \tag{36}$$

where, h_x represents the local convective heat transfer coefficient. The Nusselt number, Nu_0 , in a fully developed smooth channel at the same Reynolds number can be presented as [33]

$$Nu_0 = 0.023 Re^{0.8} Pr^{0.4} \quad \text{for heating} \tag{37}$$

3. NUMERICAL SOLUTION

The Commercial CFD software Fluent 6.3 [34] was used to simulate the fluid flow and heat transfer fields. As a part of the same package, a preprocessor Gambit was used to generate the required mesh for the solver. A non-uniform grid in the two-directions is employed. The grid density was kept higher in the vicinity of the heated wall and the baffles to capture the variations in the flow and temperature fields within the hydraulic and thermal boundary layers.

The governing equations were discretized by the Quick-scheme, decoupling with the Simple-algorithm and solved using a finite volume approach, details of which can be found in Patankar [35]. For closure of the equations, the LRN $k-\varepsilon$ model based on Jones and Launder [28] was used in the present investigation. Non-slip boundary condition is adopted on the wall. And to accurately simulate the flow in the near-wall region, the standard wall function method [29] is used.

To examine the effect of the grid size on the numerical solution, various grid systems are tested and a grid system of 260×95 (in X and Y directions respectively) is chosen in view of saving computation time. The same mesh system was used for all cases. The convergence criterion is that the normalized residuals are less than 10^{-7} for the flow equations and 10^{-9} for the energy equation.

4. RESULTS AND DISCUSSION

4.1 Numerical validation

Numerical results are compared with experimental data of Demartini *et al.* [21], who studied the baffles with a plane form for the velocity inlet $U_{in} = 7.8 \text{ m/s}$ (for $Re = 8.73 \times 10^4$). In that study, the numerical simulations were conducted in a two dimensional domain, which represents a rectangular duct of $L = 0.554 \text{ m}$ long and $H = 0.146 \text{ m}$ height, provided by two flat baffles, through which a steady flow of turbulent air.

The first baffle is attached to the upper wall of the channel at distance of $L_1 = 0.223 \text{ m}$ and the second inserted to the lower wall at 0.375 m from the entrance. The distance between the top of the baffle and the wall mother attachment is $h = 0.08 \text{ m}$. The distance between the second baffle and the exit section of the channel is $L_2 = 0.179 \text{ m}$. The distance between baffles is $P_i = 0.142 \text{ m}$. The thickness of baffles is $W_b = 0.01 \text{ m}$. Finally, the hydraulic diameter of the channel, D_h equal to 0.167 m .

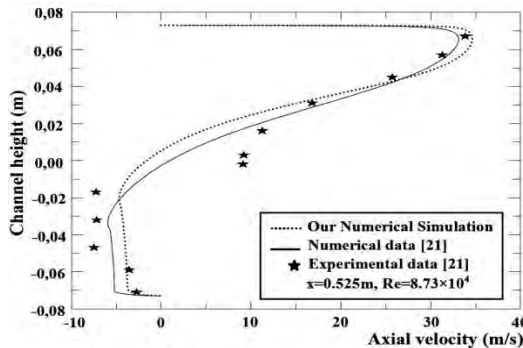


Fig. 2: Validation plot of axial velocity profiles with reported data

The comparison is shown in figure 2 for validation of the axial velocity profile distribution at the position given by $X = 0.525$ m, 0.029 m before the channel outlet. As seen in this figure, there is a good agreement between the present computation and previous work [21]. This comparison gives the confidence that the numerical model used is accurate.

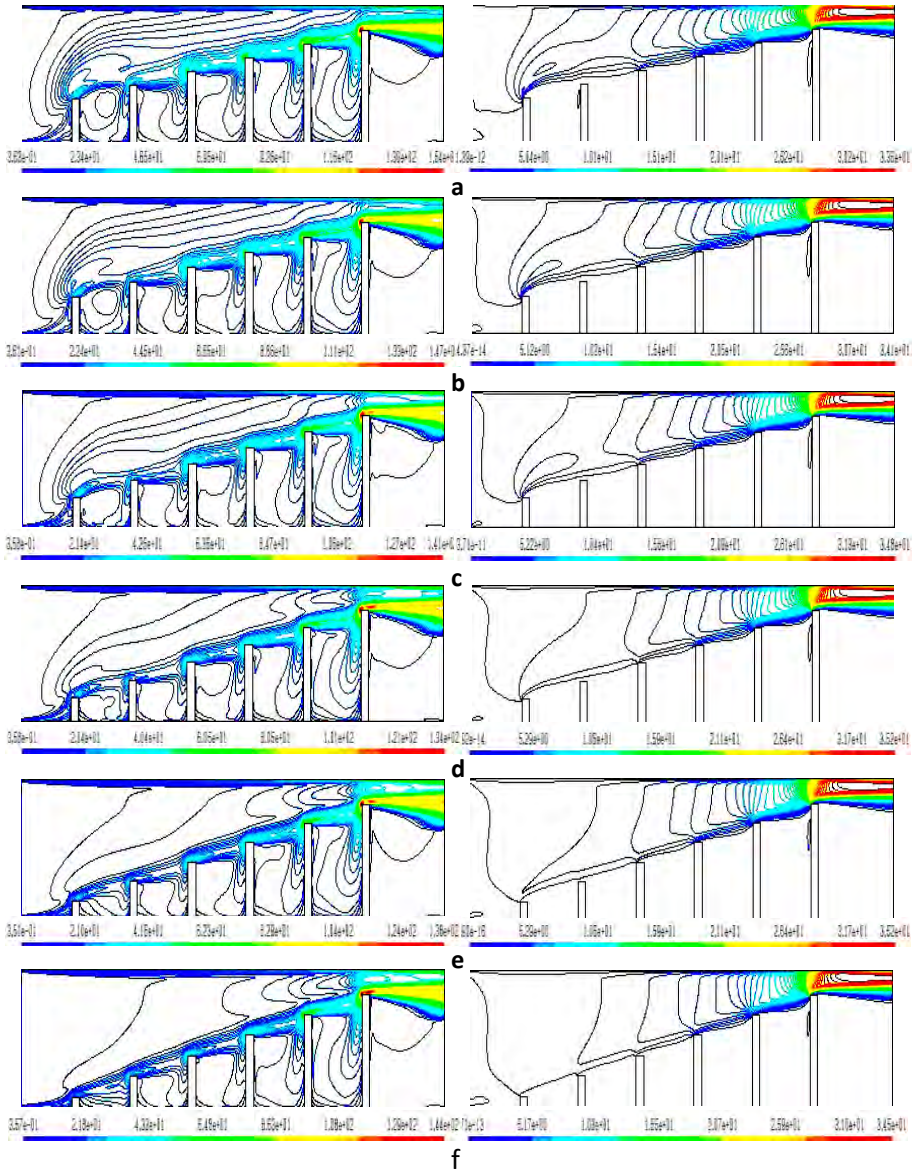


Fig. 3: Variation plots of axial velocity fields and streamlines with GBR for $Re= 12000$

a- $GBR = 0.10$, b- $GBR = 0.11$, c- $GBR = 0.12$

d- $GBR = 0.13$, e- $GBR = 0.14$, f- $GBR = 0.15$

4.2 Fluid flow structure

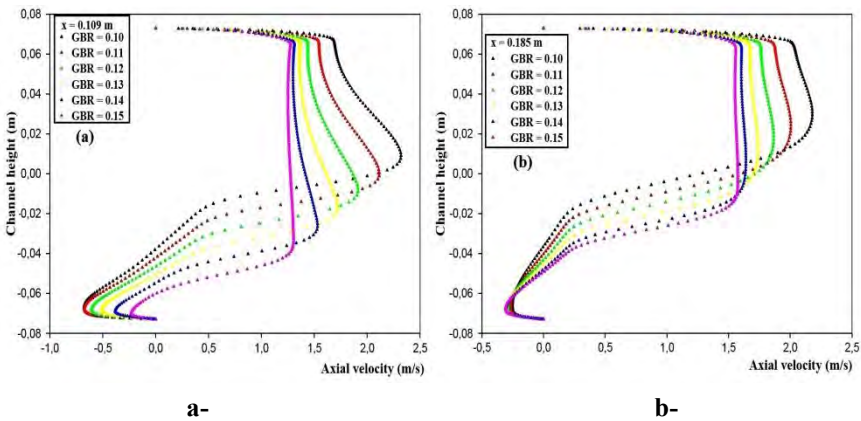
The airflow characteristics in the constant temperature-surfaced rectangular cross section channel with six baffle plates placed on the lower wall with in-line arrangement

are presented in terms of axial velocity fields and streamlines for $Re = 12000$ in the case of six different graded baffle ratio configurations ($GBR = 0.10, 0.11, 0.12, 0.13, 0.14,$ and 0.15) as shown in figure 3a-f-, respectively. The peak velocity values are seen on the upper part of the channel near the heated top surface with an acceleration process that starts just after the last lower wall-mounted baffle plate ($GBR = 0$), while the fluid velocity is observed to be very low at the lower part of the channel adjacent to the in-line graded baffle plates.

Downstream of the first baffle plate there is appearance of a vortex which tends to decrease in size and even disappear while going to the case of graded height baffles with $GBR = 0.15$. This compartment is due to the decrease of the baffle plate size which results in a reduction of the resistance to the airflow and less disturbed stream functions. In all cases, vortices with very low velocity values are observed downstream from each baffle plate, which were induced due to the flow separation. As expected, the maximum vortex height was found at $GBR = 0.10$, which decreased with an increase in GBR .

The effect of graded baffle ratios ($GBR = 0.10, 0.11, 0.12, 0.13, 0.14,$ and 0.15) on the structure of the near wall flow and on the generation of vortices in terms of axial velocity profiles is illustrated in figure 4a-f- at various axial locations, $X = 0.109\text{ m}, 0.185\text{ m}, 0.261\text{ m}, 0.337\text{ m}, 0.413\text{ m},$ and 0.500 m , respectively. Here the velocity profiles around the baffles are presented at $Re = 12.000$. It can see from this figure and for these locations that as the airflow approaches the graded baffles, its velocity is reduced in the lower part of the channel, while in the upper part is increased. Between and downstream the baffles on the lower part of channel there is appearance of larger vortices whose size changes with the graded baffle ratio.

The vortex height is approximately equal to the extent of the flow blockage by the graded baffle plates. The figure shows that the airflow velocity in the locations corresponding to the zones of counters rotating flow is significantly low as compared to that in the same regions of no baffles. For using the baffles, the increase in the GBR value gives rise to the reduction of airflow velocity value, and thus, the $GBR = 0.10$ provides maximum velocity value at all locations. The value of the u -velocity component for air flowing in the baffled channel with $GBR = 0.10$ is found to be about $1.007 - 1.097; 1.016 - 1.212; 1.024 - 1.347; 1.032 - 1.515;$ and $1.041 - 1.779$ times higher than that for $= 0.11, 0.12, 0.13, 0.14,$ and 0.15 , respectively, depending on the reference positions.



a-

b-

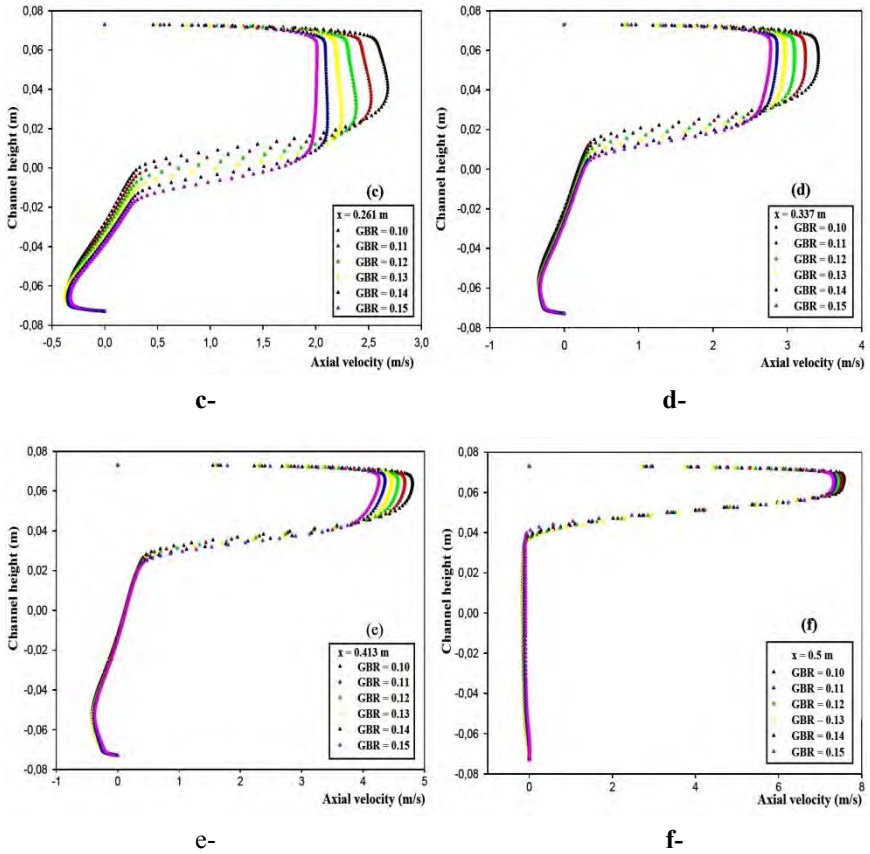
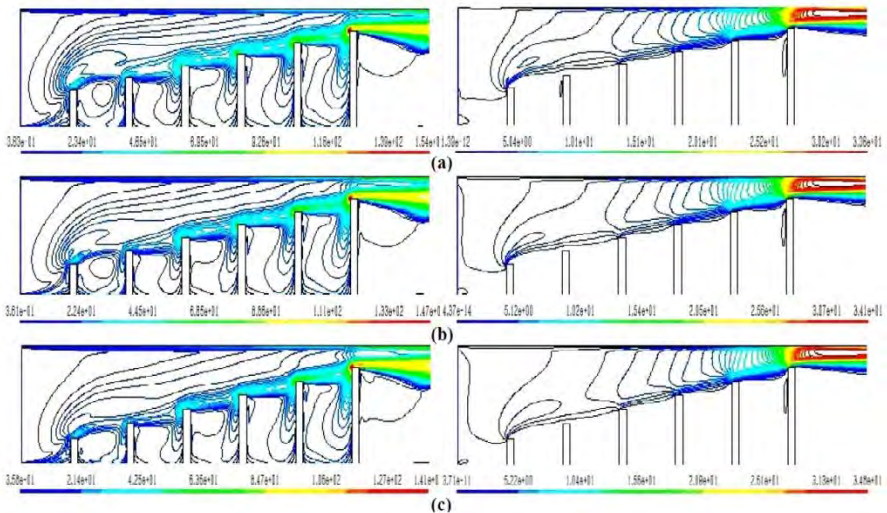


Fig. 4: Variation plots of axial velocity profiles with GBR for positions: **a-** $x = 0.109$ m, **b-** $X = 0.185$ m, **c-** $X = 0.261$ m, **d-** $X = 0.337$ m, **e-** $X = 0.413$ m, and **f-** $X = 0.500$ m, measured downstream of the entrance, $Re = 12000$



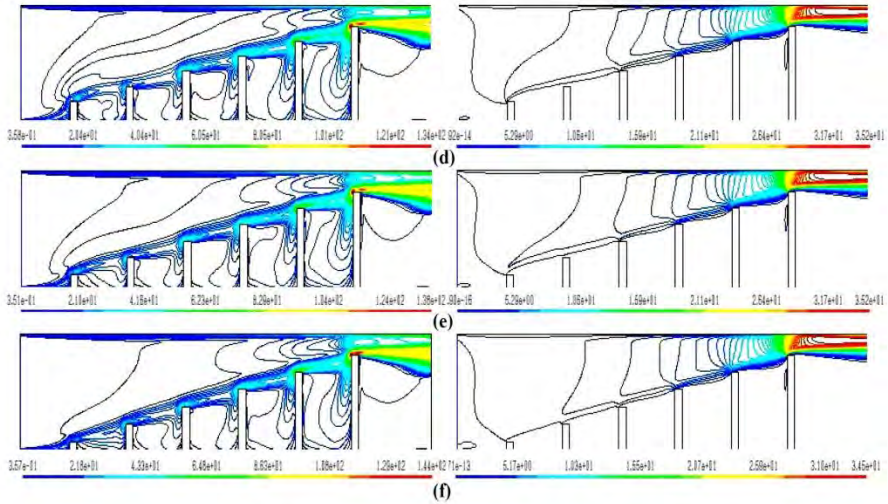


Fig. 5: Variation plots of turbulence intensity and dynamic pressure fields with GBR for $Re= 12.000$

- a-** GBR = 0.10, **b-** GBR = 0.11, **c-** GBR = 0.12
d- GBR = 0.13, **e-** GBR = 0.14, **f-** GBR = 0.15

The presence of the in-line lower wall-mounted graded baffle plates influences not only the velocity and streamline fields but also the turbulence intensity and pressure distributions in the whole domain examined. Figure 5a-f shows the contour plot turbulent intensity (TI) and dynamic pressure fields for the cases of 0.10, 0.11, 0.12, 0.13, 0.14, and 0.15 graded baffle plates at $Re= 12000$, respectively. The comparison of turbulence intensity field contour plots at different GBRs when Re is kept at a constant value shows that as the airflow is deformed near the obstacles and accelerated toward the gap above the graded baffles, a large turbulence intensity zone is formed at the upper part of the left corner and top face of the last baffle plate ($GBR = 0$) due to the high flow momentum in those regions with an acceleration process that starts just after the considered baffle.

The trends of TI are similar for all GBR values. The TI values show the largest value near the tip of the baffle plates due to the strong velocity gradients in that region and the smallest value in the regions corresponding to the zones of counter rotating flow as seen in the figure. The two-dimensional dynamic pressure contours obtained for different values of GBR are also shown in figure 5.

Similarly to the axial velocity field distribution results in figure 3, the highest values are found in the region opposite the last lower wall baffle ($GBR = 0$) near the upper channel wall for all cases, due to the high velocities in that region.

4.3 Heat and flow friction characteristics

Figure 6a-f- shows the contour plots of temperature field distributions for air flow in the constant temperature-surfaced rectangular cross section channel with six different graded baffle plate ratios ($GBR = 0.10, 0.11, 0.12, 0.13, 0.14,$ and 0.15) when $Re= 12000$. The plots show very high temperature values adjacent to the graded baffle plates for all the cases. Between and downstream the in-line graded baffle plates, recirculation cells with very high temperature values are observed.

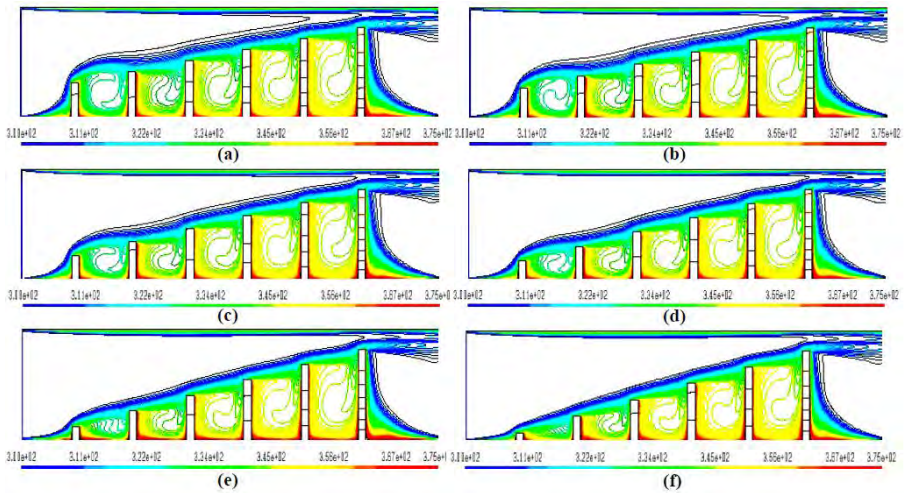


Fig. 6: Variation plots of fluid temperature contours with GBR for Re= 12.000

- a- GBR = 0.10, b- GBR = 0.11, c- GBR = 0.12
- d- GBR = 0.13, e- GBR = 0.14, f- GBR = 0.15

In the region opposite the baffle tip along the heated top channel wall, the temperature gradient is increased, due to the high velocities in that region. Due to the change in the airflow direction produced by the lower wall baffle presence with the GBR range studied, the highest temperature values appear in the lower part of the channel behind the bottom wall with an acceleration process that starts just after the last baffle (GBR = 0).

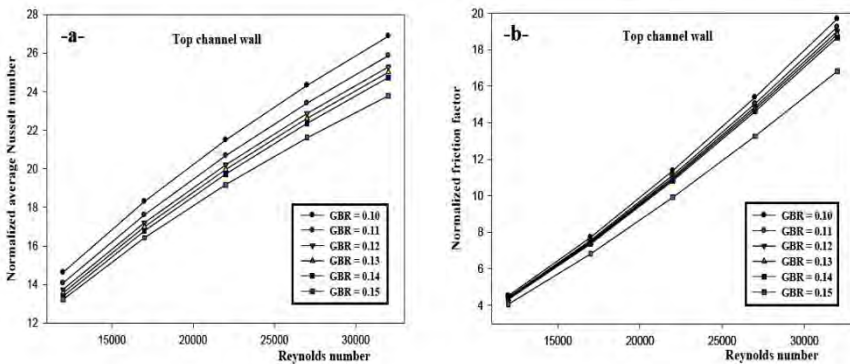


Fig. 7: Variation of a- Nu_{av}/Nu_0 and b- f/f_0 with Re for various GBRs

Figure 7a- and b- shows the variation of the average Nu_{av}/Nu_0 ratio and friction factor ratio, f/f_0 with different Re numbers (12000-32000) at the surface of the top channel heated wall and various GBR values, respectively. In general, Nu_{av}/Nu_0 and f/f_0 values tend to increase with the rise of Reynolds number for all graded baffle height cases. As seen from figure 7a-, the use of the in-line lower-wall graded baffle plates lead to a substantial increase in the heat exchange ratio over the plain channel with no baffle, due to the induction of high vortex downstream from each baffle plate close to the bottom solid wall and thin hydraulic and thermal boundary layers in the

baffled channel, leading to higher vortex strength, turbulence intensity and temperature gradients, enhancing the heat transfer.

The average increase in Nu_{av}/Nu_0 of the graded baffled channel is in a range of 13.217 - 26.888 times above the smooth channel, depending on the GBR and Re values. For using the graded baffle plates, the trends of Nu_{av}/Nu_0 are similar for all GBR values. The heat transfer rate shows a decrease trend with increasing the GBR value for all Reynolds numbers used and thus, the GBR = 0.10 provides maximum Nu_{av}/Nu_0 value.

For the in-line graded baffles and for this Re range (12000 - 32000), the increases in the normalized average Nusselt number with the GBR = 0.10, 0.11, 0.12, 0.13, 0.14 and 0.15 are in the range of 14.623 - 26.888, 14.070 - 25.877, 13.735 - 25.286, 13.556 - 25.013, 13.378 - 24.741, and 13.217 - 23.794 times above the no baffle case, respectively. Also, the use of graded height baffles at GBR = 0.10 gives higher heat transfer than that with GBR = 0.11, 0.12, 0.13, 0.14 and 0.15 around 3.761 - 3.779%, 5.960 - 6.074%, 6.973 - 7.295%, 7.987 - 8.516% and 9.612- 11.508%, respectively. In Figure 7b-, it is found that the normalized friction factor decreases with increasing the GBR ratio, apart from Re values.

This is because the increase of the graded baffle height ratio and the diminution of their height as well as their size, by going from the GBR = 0.10 to the GBR = 0.15, reduces the resistance to the airflow and so leads to a decrease of the friction loss in the channel. The graded baffle in the case of GBR = 0.10 gives the highest f/f_0 and while the one with GBR = 0.15 provides the lowest for all Reynolds numbers. The f/f_0 values for the channel with graded baffles appear to be about 4.059 - 19.680 times above those for the plain channel with no baffle, depending on the GBR and Re values.

For the range of investigation, the f/f_0 value at GBR = 0.10 is found to be around 2.061 - 2.267%, 2.998 - 3.466%, 3.725 - 4.316%, 4.453 - 5.167%, and 10.217 - 14.565% higher than that at GBR = 0.11, 0.12, 0.13, 0.14, and 0.15, respectively. The friction loss of graded baffle plates with GBR = 0.15 is lower than that of graded baffle plates with GBR = 0.10 - 0.14, which indicates that the 0.15 graded height baffle is more advantageous than the others.

5. CONCLUSION

This paper presents fluid flow configurations and heat and friction loss transfer characteristics in a constant temperature-surfaced rectangular channel with in-line lower wall-mounted baffle plates. Turbulent and incompressible flow of fluid circulating through the channel is assumed. The mesh was generated by the pre-processor software Gambit 2.3. The two-equation low-Reynolds number $k-\epsilon$ turbulence model is employed to simulate the turbulent transport quantities and close the solving problem.

The Finite Volume Method by means of Commercial CFD software FLUENT 6.3 was applied in this research work. The effects of graded baffle geometries (GBR = 0.10, 0.11, 0.12, 0.13, 0.14, and 0.15) as well as Reynolds numbers (Re = 12000, 17000, 22000, and 32000) are examined.

The airflow structure is affected by the gradation of these baffle plates, resulting in the formation of vortices downstream from each baffle plate. The size of these vortices strongly depend on the graded baffle height ratio and the Reynolds number. This flow

structure has profound influences on the heat and friction loss characteristics. It is observed that apart from the rise of Reynolds number, the increase in the graded baffle height ratio leads to a decrease in the heat exchange rate and skin friction loss. The graded baffled channel with $GBR = 0.10$ gives the highest Nu_{av}/Nu_0 and f/f_0 while the one with $GBR = 0.15$ provides the lowest.

This is because the graded baffle plate in the case of $GBR = 0.10$ can induce larger vortex appearing behind the baffle plate than the one with lower GBR and the smooth channel. The heat transfer rate and friction loss values for the channel with graded baffle plates appear to be about 13.217 - 26.888 and 4.059 - 19.680 times above those for the channel with no baffle, respectively, depending on the GBR and Re values.

Author’s Contributions- Each author of this manuscript made considerable contributions in developing the mathematical modeling, data-analysis and contributed to the writing of this manuscript.

NOMENCLATURE

C_f , Skin friction coefficient	f , Friction factor
$C_{1\varepsilon}$, Constant used in the standard k- ε model	f_1, f_2, f_μ , Modeling damping functions used for the LRN k- ε model
$C_{2\varepsilon}$, Constant used in the standard k- ε model	G , Production rate of the kinetic energy, m^2/s^2
C_μ , Constant used in the standard k- ε model	GBR , Graded baffle ratio
D_h , Hydraulic diameter of the rectangular channel, m	G_{hb} , Graded height baffle, m h , Baffle height, m
H , Height of air tunnel in channel, m	k , Turbulent kinetic energy, m^2/s^2
h_x , Local convective heat transfer coefficient, $W/m^2 K$	L , Channel length, m Re , Reynolds number
L_{in} , Distance upstream of the first baffle, m	L_{out} , Distance downstream of the second baffle, m
Nu_x , Local Nusselt number	Nu_{av} , Average Nusselt number
Nu_0 , Average Nusselt number in smooth channel at the same Reynolds number	P , Fluid pressure, Pa Pr , Prandtl number
P_{atm} , Atmospheric pressure, Pa	R_T , Constant used in the LRN k- ε model
S , Baffle distance or spacing, m	R_y , Constant used in the LRN k- ε model
T , Temperature, K	T_{in} , Inlet temperature, K
T_w , Wall temperature, K	U_{in} , Inlet velocity, m/s
\bar{U} , Channel average velocity, m/s	u , Fluid velocity in the x-direction, m/s
W , Channel width, m	v , Fluid velocity in the y-direction, m/s
w , Baffle thickness, m	x, y , Cartesian coordinates, m
y^+ , Dimensionless distance to the wall	Γ_ϕ , Coefficient of turbulent diffusion
ε , Turbulent dissipation rate, m^2/s^3	λ_f , Thermal conductivity of fluid, $W/m \text{ }^\circ C$
μ , Dynamic viscosity, kg/ms	λ_s , Thermal conductivity of solid, $W/m \text{ }^\circ C$
μ_e , Effective viscosity, kg/ms	μ_l , Laminar viscosity, kg/ms
ν , Kinematics viscosity, kg/ms	ρ , Fluid density, kg/m^3

σ_K , Constant used in the standard k- ϵ model	σ_ϵ , Constant used in the standard k- ϵ model
σ_T , Constant used in the standard k- ϵ model	τ_w , Wall shear stress, Pa
ϕ , Stands for the dependent variables u, v, T, k and ϵ	ΔP , Pressure drop, Pa
Atm, Atmospheric; e, Effective,	S_ϕ , Limit of source for the general variable ϕ
l, laminar; t, Turbulent	f, fluid; in, Inlet of the channel, s, solid; w, Wall

REFERENCES

- [1] J. Anotoniou and G. Bergeles, 'Development of the Reattached Flow Behind Surface-Mounted Two-Dimensional prisms', Journal of Fluids Engineering, Vol. 110, N°2, pp. 127 - 133, 1988.
- [2] C. Berner, F. Durst and D.M. McEligot, 'Flow Around Baffles', Journal of Heat Transfer, Vol. 106, N°4, pp. 743 - 749, 1984.
- [3] B.H.L. Gowda, B.A.A. Achar, M. Hasan and K. Prasanna Kumar, M. Shuja, T.L.S. Rao and D. Sen. 'Flow Field Around Baffles in a Rectangular Enclosure - A Flow Visualization Study', In: proceeding of 37th National & 4th International Conference on Fluid Mechanics and Fluid Power; 2010 Dec 16-18; IIT Madras, Chennai, India; 2010.
- [4] M.A. Habib, A.M. Mobarak, M.A. Sallak, E.A. Abdel Hadi and R.I. Affify, 'Experimental Investigation of Heat Transfer and Flow Over Baffles of Different Heights', Transactions ASME Journal of Heat Transfer, Vol. 116, N°2, pp. 363-368, 1994.
- [5] Y.L. Tsay, T.S. Chang and J.C. Cheng, 'Heat Transfer Enhancement of Backward-Facing Step Flow in a Channel by Using Baffle Installed on the Channel Wall', Acta Mechanical, Vol. 174, N°1, pp. 63-76. 2005.
- [6] Nasiruddin and M.H. Kamran Siddiqui, 'Heat Transfer Augmentation in a Heat Exchanger Tube Using a Baffle', International Journal of Heat and Fluid Flow, Vol. 28, N° 2, pp. 318-328, 2007.
- [7] D. Sahel and R. Benzeguir, 'Friction Factor and Heat Transfer Optimization in a Channel with Graded Size Ribs', in: Proceeding of 16^{èmes} Journées Internationales de Thermique (JITH'013), du 13 au 15 Novembre 2013, Marrakech, Maroc, 2013.
- [8] M. Saffar-Avval and E. Damangir, 'A General Correlation for Determining Optimum Baffle Spacing for all Types of Shell and Tube Exchangers', International Journal of Heat and Mass Transfer, Vol. 38, N°13, pp. 501-2506, 1995.
- [9] H. Li and V. Kottke, 'Effect of Baffle Spacing on Pressure Drop and Local Heat Transfer in Staggered Tube Arrangement', International Journal of Heat and Mass Transfer, Vol. 41, N°10, pp. 1303-1311, 1998.
- [10] R. Karwa and B.K. Maheshwari, 'Heat Transfer and Friction in an Asymmetrically Heated Rectangular Duct with Half and Fully Perforated Baffles at Different Pitches', International Communication in Heat and Mass Transfer, Vol. 36, pp. 264-268, 2009.
- [11] R. Saim, H. Benzenine, H.F. Öztöp and K. Al-Salem, 'Turbulent Flow and Heat Transfer Enhancement of Forced Convection over Heated Baffles in a Channel:

Effect of Pitch of Baffles', International Journal of Numerical Methods for Heat and Fluid Flow, Vol. 23, pp. 613-633, 2013.

- [12] P. Dutta and S. Dutta, '*Effect of Baffle Size, Perforation, and Orientation on Internal Heat Transfer Enhancement*', International Journal of Heat and Mass Transfer, Vol. 41, pp. 3005-3013, 1998.
- [13] P. Dutta and A. Hossain, '*Internal Cooling Augmentation in Rectangular Channel Using Two Inclined Baffles*' International Journal of Heat and Fluid Flow, Vol. 26, pp. 223-232, 2005.
- [14] Y.T. Yang and C.Z. Hwang, '*Calculation of Turbulent Flow and Heat Transfer in a Porous Baffled Channel*', International Journal of Heat and Mass Transfer, Vol. 46, pp. 771-780, 2003.
- [15] K.H. Ko and N.K. Anand, '*Use of Porous Baffles to Enhance Heat Transfer in a Rectangular Channel*', International Journal of Heat and Mass Transfer, Vol. 46, N°22, pp. 4191-4199, 2003.
- [16] G.-Y. Zhou, J. Xiao, L. Zhu, J. Wang and S.-T. Tu, '*A Numerical Study on the Shell-Side Turbulent Heat Transfer Enhancement of Shell-and-Tube Heat Exchanger with Trefoil-Hole Baffles*', Energy Procedia, Vol. 75, pp. 3174-3179, 2015.
- [17] M. Bahiraei, M. Hangi and M. Saeedan, '*A Novel Application for Energy Efficiency Improvement Using Nano-Fluid in Shell-and-Tube Heat Exchanger Equipped with Helical Baffles*', Energy, Vol. 93, pp. 2229 - 2240, 2015.
- [18] B. Gao, Q. Bi, Z. Nie and J. Wu, '*Experimental Study of Effects of Baffle Helix Angle on Shell-Side Performance of Shell-and-Tube Heat Exchangers with Discontinuous Helical Baffles*', Experimental Thermal and Fluid Science, Vol. 68, pp. 48 - 57, 2015.
- [19] J. Wua, J. Zhou, Y. Chen, M. Wang, C. Dong and Y. Guo, '*Experimental Investigation on Enhanced Heat Transfer of Vertical Condensers with Trisection Helical Baffles*', Energy Conversion and Management, Vol. 109, pp. 51 - 62, 2016.
- [20] B. Kundu, K.S. Lee and A. Aziz, '*Unique Analysis for Cascaded Rectangular-Triangular Fins with Convection-Radiation Transport*', Journal of Thermophysics and Heat Transfer, Vol. 27, N°1, pp. 101-110, 2002.
- [21] L.C. Demartini, H.A. Vielmo and S.V. Möller, '*Numeric and Experimental Analysis of the Turbulent Flow through a Channel with Baffle Plates*', Journal of the Brazilian Society of Mechanical Sciences and Engineering, Vol. 26, N°2, pp. 153 - 159, 2004.
- [22] S. Sripattanapipat and P. Promvonge, '*Numerical Analysis of Laminar Heat Transfer in a Channel with Diamond-Shaped Baffles*', International Communication in Heat and Mass Transfer, Vol. 36, N°1, pp. 32-38, 2009.
- [23] F. Wang, J. Zhang and S. Wang, '*Investigation on Flow and Heat Transfer Characteristics in Rectangular Channel with Drop-Shaped Pin Fins*', Propulsion and Power Research, Vol. 1, N°1, pp. 64-70, 2012.
- [24] P. Sriromreun, C. Thianpong and P. Promvonge, '*Experimental and Numerical Study on Heat Transfer Enhancement in a Channel with Z-shaped Baffles*', International Communication in Heat and Mass Transfer, Vol. 39, N°7, pp. 945-952, 2012.

- [25] H. Benzenine, R. Saim, S. Abboudi, O. Imine, 'Numerical Analysis of a Turbulent Flow in a Channel Provided with Transversal Waved Baffles', *Thermal Science*, Vol. 17, N°3, pp. 801-812, 2013.
- [26] W. Jedsadaratanachai and A. Boonloi, 'Effects of Blockage Ratio and Pitch Ratio on Thermal Performance in a Square Channel with 30° Double V-Baffles', *Case Studies in Thermal Engineering*, Vol. 4, pp. 118-128, 2014.
- [27] W. Jedsadaratanachai, N. Jayranaiwachira and P. Promvonge, '3D Numerical Study on Flow Structure and Heat transfer in a Circular Tube with V-Baffles', *Chinese Journal of Chemical Engineering*, Vol. 23, pp. 342-349, 2015.
- [28] W.P. Jones and B.E. Launder, 'The Prediction of Laminarization with a Two-Equation Model of Turbulence', *International Journal Heat Mass Transfer*, Vol. 15, N°2, pp. 301-314, 1972.
- [29] B.E. Launder and D.B. Spalding, 'The Numerical Computation of Turbulent Flow', *Applied Mechanics and Engineering*, Vol. 3, N°2, pp. 269-289, 1974.
- [30] C.C. Chieng and B.E. Launder, 'On the Calculation of Turbulent Heat Transport Downstream from an Abrupt Pipe Expansion', *Numerical Heat Transfer*, Vol. 3, N° 2, pp. 189-207, 1980.
- [31] H.K. Versteeg and W. Malalasekera, 'An Introduction to Computational Fluid Dynamics, the Finite Volume Method', Addison Wesley Longman Limited, England, 1995.
- [32] B.S. Petukhov, 'Heat Transfer in Turbulent Pipe Flow With Variable Physical Properties', in: J.P. Harnett, Editor. *Advances in Heat Transfer*, New York: Academic Press., Vol. 6, pp. 504 - 564, 1970.
- [33] F. Incropera and P.D. Dewitt, 'Introduction to Heat Transfer', 3rd Edition, John Wiley and Sons. Inc., 1996.
- [34] Fluent Inc., 'User's Guide 6.3', Centerra Park Lebanon, USA, 2006.
- [35] S.V. Patankar, 'Numerical Heat Transfer and Fluid Flow', McGraw-Hill, New York, 1980.